JOURNAL OF MATERIALS SCIENCE 15 (1980) 1823–1831

The mechanical properties of epoxy resins

Part 2 *Effect of plastic deformation upon crack propagation*

SALIM YAMINI, ROBERT J. YOUNG
Department of Materials, Queen Mary College, Mile End Road, London E1 4NS, UK

Crack propagation in a series of epoxy resins described in Part 1 has been studied as a function of testing rate and temperature. It has been found that crack propagation is continuous at low temperatures but that as the temperature is raised the mode of propagation becomes unstable (stick/slip). Features on the fracture surfaces at the crack arrest lines have been shown to be of the same dimensions as those expected for a Dugdale plastic zone. It has been suggested that the "slip" process takes place by slow growth of a crack through the plastic zone followed by rapid propagation through virgin material. It has been shown that the stick/slip behaviour is due to blunting of the crack which is controlled by the yield behaviour of the resin. A unique fracture criterion has been shown to be applicable to epoxy resins which is that a critical stress of the order of three times the yield stress must be achieved at a critical distance ahead of the crack. Electron microscope replicas of the fracture surfaces have been obtained and an underlying nodular structure can be resolved. However, no direct correlation between the nodule size and fracture properties has been found.

1. Introduction

There is currently a great deal of interest in the mechanisms of crack propagation in brittle polymers. The general subject of crack propagation in thermosetting polymers has been reviewed recently by one of the authors [1] and this particular paper is concerned with the propagation of cracks in epoxy resins.

In certain polymers such as polymethylmethacrylate (PMMA) cracks tend to propagate in a stable, continuous way through a constant crack-opening displacement (δ_c) criterion [2, 3], whereas in other polymers such as epoxy resins [4], crack propagation tends to occur in an unstable stick/slip manner. It is known [5] that unstable propagation is suppressed in epoxy resins if the cracks are propagated at low temperatures, when the material is well below its T_g. It has been shown recently [6] that under these conditions a constant δ_c criterion also holds for an epoxy resin. It has been recognized for several years that there is a relationship between the crack propagation behaviour and the plastic flow properties of an epoxy resin [6, 7] but it is only very recently that quantitative theories have been developed to account for this relationship. Following a suggestion from Williams [8], the authors have been able to show that stick/slip propagation in one particular epoxy resin system could be explained through a crack blunting mechanism [9]. The same approach has been developed more formally by Kinloch and Williams [10] who found that the crack blunting mechanism could successfully explain the modes of crack propagation in a wide variety of epoxy resins.

The plastic deformation of a series of epoxy resins has been carefully investigated in Part 1 and explained in terms of current theories of plastic deformation in glassy polymers. In this second paper the relationship between the flow behaviour and crack propagation has been analysed in detail as a function of the amount of curing agent used with the resin and post-cure temperature.

2. Experimental

The epoxy resin used in this study was Epikote 828 hardened with different amounts of triethylenetetramine (TETA) and cured for 3 h at dif-

0022–2461/80/071823–09$02.90/0

ferent temperatures as described in a previous publication [5]. The crack propagation was studied using the double torsion (DT) test which is described in detail elsewhere [11, 12]. This test is particularly useful since the critical stress intensity factor K_{IC} is proportional to the load needed to propagate the crack [11]. For the DT tests 3.9 mm sheets of resin were used and they were deformed in the environmental chamber of an Instron mechanical testing machine.

The fracture surfaces were examined in reflected light in an optical microscope. Features on the fracture surface were measured from photographs taken at standard calibrated magnifications. Two-stage replicas of the fracture surfaces were also made using polyacrylic acid (PAA). A few drops of the PAA were placed in the areas of interest in the fracture surface and allowed to dry. The PAA was then removed, shadowed with gold–palladium and coated with carbon. The shadowed carbon film was removed from the PAA by floating the coated replica upon water. The replicas were examined in a JEOL JEM-7 electron microscope operated at 80 kV.

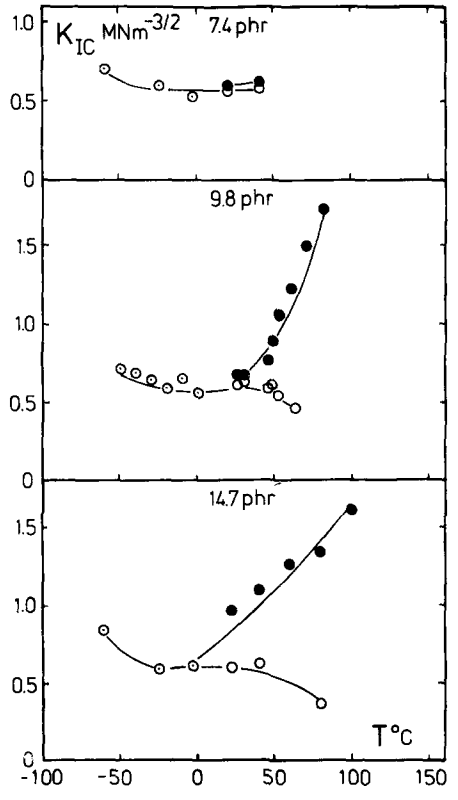

Figure 1 Variation of K_{IC} with testing temperature for epoxy resins containing different amounts of TETA. The cross-head speed used was 0.5 mm min^{-1}. • K_{ICi}, ○ K_{ICa}, ⊙ K_{IC} continuous.

3. Results

3.1. Crack propagation

Most of the results of crack propagation experiments used in this present paper have been given in previous publications [5–7, 9, 12]. The only data used that have not been presented before are given in Fig. 1. This shows the variation of K_{IC} with temperature for the Epitoke 828 hardened with different amounts of TETA. It can be seen that in each case propagation is continuous at low temperatures ($K_{ICi} = K_{ICa}$) whereas when the temperature is raised crack jumping takes place ($K_{ICi} > K_{ICa}$). The size of the crack jump increases as the temperature approaches the T_g of the resin (Part I). In the case of the resin containing only 7.4 phr hardener, the T_g is very low (~ 63° C) and DT tests could not be carried out much above room temperature.

3.2. Fractography

It has been found in earlier investigations [7, 13] that there are several characteristic features that can be seen on the fracture surfaces of epoxy resins. When crack propagation is continuous the surface tends to be relatively smooth and featureless. On the other hand, when stick/slip propagation takes place there are crack arrest features on the surface. These features fall into three main categories; namely, triangular markings, fine arrest lines and broad rough area [7]. The presence of each type of feature depends upon the state of cure of the resin and the temperature of testing.

The triangular markings are typically found in under-cured resins [7] (i.e. low curing temperature and/or small amounts of curing agent). They appear adjacent to crack arrest lines as shown in Fig. 2a. The electron micrograph in Fig. 2b is obtained from the vicinity of a crack arrest line on the same specimen. It can be seen that the surface features are streaked in the crack propagation direction and that there is an underlying nodular structure on the scale of ~ 1000 Å. There is also a broad band along the crack arrest line.

Fine arrest lines are found in specimens just undergoing the transition from stable to unstable propagation. Fig. 3 shows an optical micrograph and an electron micrograph of the fracture surface of a specimen cured with 9.8 phr TETA and heated for 3 h at 100° C which has been fractured

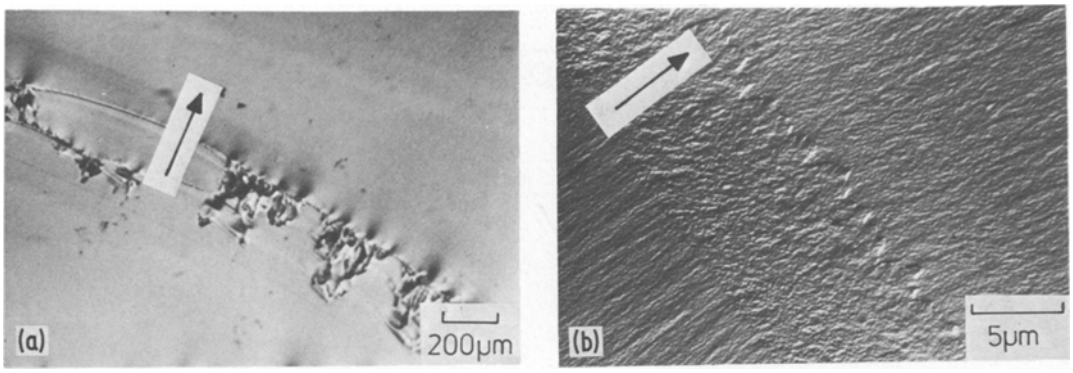

Figure 2 Fracture surfaces of an epoxy resin cured with 9.8 phr TETA. The specimen was post-cured at 50° C for 3 h and tested at a cross-head speed of 0.05 mm min^{-1} at 22° C. (a) Optical micrograph of surface. (b) EM replica of crack arrest line. (Crack growth direction indicated by arrows).

at room temperature. Fig. 3a shows that the specimen has a fine arrest line. The electron micrograph in Fig. 3b shows the arrest line at a higher magnification. It can be seen that the structure is again streaked and the arrest line corresponds to an abrupt change in direction of the streaks. There appears to be an underlying nodular structure of the scale of ~ 500 Å.

A good example of a broader type of crack arrest line is given in Fig. 4a. This type of feature is typical of well cured specimens fractured at temperatures close to T_g [7]. The fracture surface is featureless until the crack arrest point. After crack arrest there is a slow growth region [13] of closely spaced striations parallel to the crack growth direction. Following the slow growth region there is a rougher hackled region where the crack accelerates during the "slip" process. Examination of the fracture surface by EM replicas has shown that the smooth areas of such specimens are relatively featureless in contrast to the slow-growth region which is shown in Fig. 4b. In this area there are V-shaped features which appear to be caused by the crack propagating on different levels. It was not possible to resolve any underlying nodular structure on the specimen used in Fig. 4.

3.3. Slow-growth region

It was pointed out in the previous section that in well-cured specimens fractured at high temperatures there is a characterisitc region of slow crack growth which was first identified by Phillips *et al.* [13]. It is found that the size of this region, l_r, increases as the temperature of testing is raised. This can be seen clearly in Fig. 5 for a resin containing 14.7 phr TETA, where micrographs are given for specimens which have been fractured at two different temperatures. It was shown in Fig. 1 that for this formulation the critical stress intensity factor for crack initiation K_{ICi} also increases

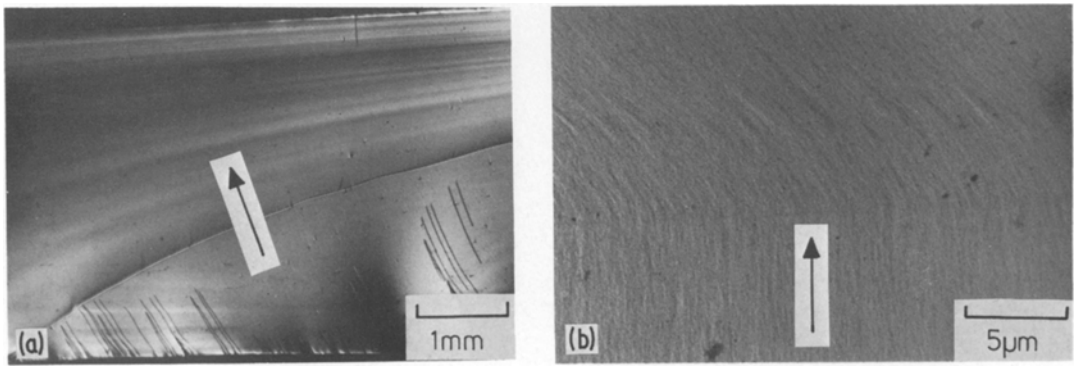

Figure 3 Fracture surface of an epoxy resin cured with 9.8 phr TETA. The specimen was post-cured at 100° C for 3 h and tested at a cross-head speed of 0.05 mm min^{-1} at 22° C. (a) Optical micrograph of fracture surface. (b) EM replica of crack arrest line. (Crack growth direction indicated by arrows.)

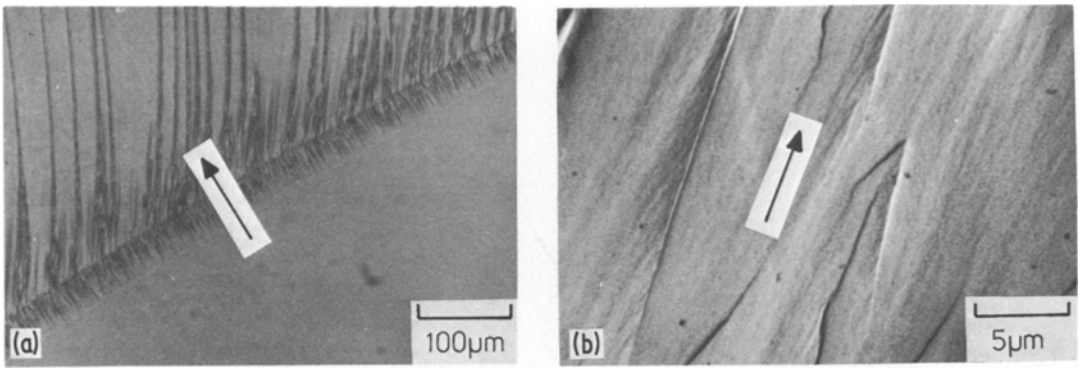

Figure 4 Fracture surface of an epoxy resin cured with 9.8 phr TETA. The specimen was post-cured at 150° C for 3 h and tested at a cross-head speed of 5 mm min^{-1} at 22° C. (a) Optical micrograph of fracture surface. (b) EM replica of slow growth region following the crack arrest line. (Crack growth direction indicated by arrows).

with increasing temperature. Fig. 6 shows that there is a unique correlation between the length of the slow growth regime, l_r and K_{ICi} for different formulations tested under a variety of experimental conditions. The significance of this will be discussed later.

4. Discussion

4.1. Mechanisms of crack propagation

It has long been recognized that crack propagation in thermoplastics such as PMMA takes place by the breakdown of crazes [2]. There have also been suggestions that crazing occurs in thermosetting polymers such as epoxy resins [14, 15]. It is unlikely in fully cured materials that the amount of local tensile drawing required to form a craze would be possible and recent experimental observations [16] have tended to suggest that crazing does not occur. It has also been suggested that epoxy resins have a nodular structure and that this affects the mechanisms of crack propagation [16]. The observations in Section 3.2 may help to shed some light on both crazing and the effect of the nodular structure.

It is clear from the electron micrographs in Figs. 2 to 4 that there is no evidence of craze debris on the surface of these epoxy resins. This is in agreement with Mijovic and Koutsky [16] who came to a similar conclusion for DETA-cured epoxy resins. We would therefore strongly disagree with Morgan and O'Neal [14] concerning crazing in epoxy resins. There now appears to be overwhelming evidence against crazing in bulk specimens of these polymers.

Koutsky and co-workers [16, 17] have recently been concerned with the effect on nodules upon the properties of epoxy resins. The existence of nodules in glassy polymers is a matter of some controversy with Uhlmann [18] suggesting that they are artefacts and Yeh [19] and co-workers

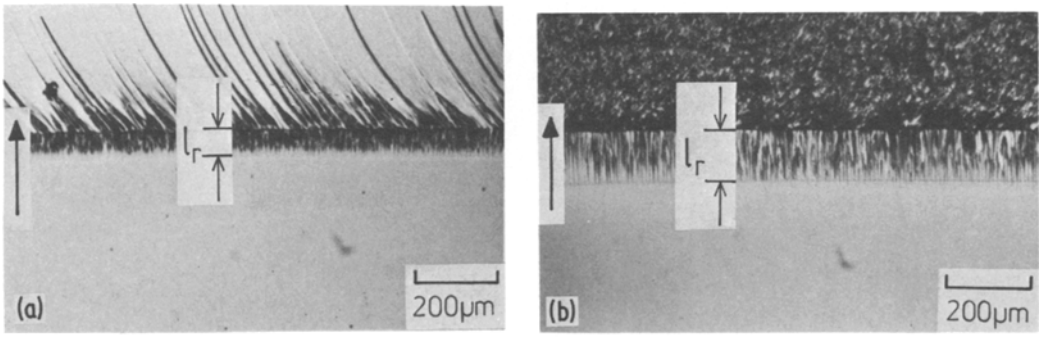

Figure 5 Optical micrographs of the crack arrest region on fracture surfaces of an epoxy resin hardened with 14.7 phr TETA and post-cured for 3 h at 100° C. The length of the slow-growth region is given by l_r. (a) Specimen fractured at 22° C using a cross-head speed of 0.5 mm min^{-1}. (b) Specimen fractured at 60° C using a cross-head speed of 0.5 mm min^{-1}.

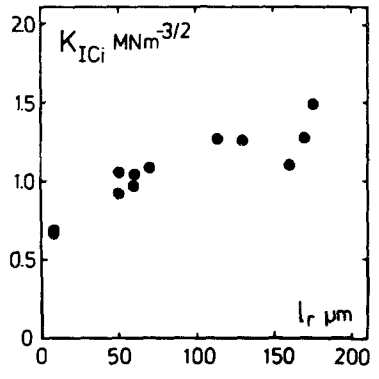

Figure 6 Plot of K_{ICi} against l_r for the specimens used in Fig. 5 and other formulations of resin tested at different rates and temperatures.

affirming that they are a representation of the true structure of amorphous polymers. Although we have no wish to become involved in this arguement we feel that the results of small-angle X-ray scattering [18] strongly suggest that the nodular structure is an artefact in glassy thermoplastics. However, even Uhlmann suggests [18] that the SAXS evidence is more ambiguous in epoxy resins and that there could be inhomogeneities which give rise to the nodular structure observed on fracture surface replicas. In fact, since epoxy resins are hardened by the addition of a curing agent, a two-phase structure would appear to be highly likely. Mijovic and Koutsky [16] have shown that the nodule size decreases with an increase in the curing agent concentration for a DETA cured resin, post-cured at the same temperature and for identical periods of time. The micrographs in Figs. 2 to 4 clearly show that the nodule size is also affected by the post-cure temperature when the same concentration of curing agent is used. In the under-cured resin (Fig. 2) the nodules are of the order of 1000 Å diameter and their size decreases dramatically as the temperature of the cure is raised (Figs. 3, 4). It is known that the mechanical properties of the resin are affected by the post-cure temperature [7]. The question that must be asked is does the size of the nodules directly affect the mechanical properties, or are both of these variables controlled by the amount of curing agent used and the post-cure temperature but are, in fact, independent of each other? Mijovic and Koutsky [16] strongly ascertain that the mechanical properties are controlled by the morphology of the polymer and in particular the nodule size. They show that G_{ICi} varies continuously with nodule size and has a maximum value at a nodule diameter of ~ 300 Å. They do not explain why G_{ICi} should peak at this diameter and we feel that such a correlation is fortuitous and does not yet prove that the morphology is controlling the mechanical properties. Nevertheless we think that this approach to the structure/property relations in epoxy resins is useful.

4.2. Plastic deformation at the crack tip

It is clear that plastic deformation must occur at the crack tip during crack propagation in epoxy resins [6, 9, 10]. However, it is extremely difficult to show directly that plastic deformation has taken place. It is possible to see blunt cracks with with crack tip radii of the order of several microns [10] but observation of plastic zones, which may be present, has proved extremely difficult. It has been shown by Phillips *et al.* [13] that when stick/slip propagation occurs in epoxy resins there is a characteristic slow-growth region after the crack arrest line. They observed the growth of a crack in an epoxy sample and found that after the "slip" process the crack became stationary at the arrest line. They observed that prior to the next "slip" process it grew slowly through a small region similar to those shown in Fig. 5 before bursting through and jumping ahead. Fig. 6 shows that there is a clear correlation between the size of the slow growth region, l_r and K_{ICi}. In fact, rough calculations showed that for most specimens showing this feature l_r was approximately the same value as the radius of a Dugdale plastic zone r_p calculated using the equation [21].

$$r_p = \frac{\pi}{8}\left(\frac{K_{IC}}{\sigma_y}\right)^2 \quad (1)$$

where σ_y is the yield stress of the material. Fig. 7 is a plot of $(K_{ICi}/\sigma_y)^2$ against l_r using the data in Fig. 6. The values of σ_y have been taken from Part 1 and previous publications [6, 12]. The straight line in Fig. 7 is drawn with a slope of $8/\pi$ (~ 2.55) and represents the relationship between r_p and $(K_{ICi}/\sigma_y)^2$ if a Dugdale plastic zone is present at the crack tip. It can be seen that there is a certain amount of scatter but the plot does imply that the length of the slow-growth region l_r is closely related to r_p.

A clear picture of stick/slip propagation now emerges. It appears that during the loading after crack arrest a plastic zone forms at the tip of the crack. Propagation then takes place by slow

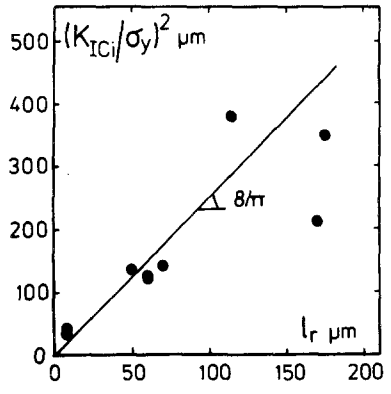

Figure 7 Plot of $(K_{ICi}/\sigma_y)^2$ against l_r using some of the data from Fig. 6. The straight line is drawn with a slope of $8/\pi$ according to Equation 1 assuming that $l_r \approx r_p$.

growth through the plastic zone followed by rapid propagation through virgin material. The slow-growth region therefore defines the size of the plastic zone at the crack tip and the characteristic V-shaped marking in this area (Fig. 4b) are due to slow crack growth through a plastically deformed region. Although this is only indirect evidence of the presence and size of the plastic zone it gives an important new insight into the processes taking place at the crack tip.

4.3. Crack blunting

Several years ago it was suggested [6] that it may be possible to explain stick/slip propagation by a crack blunting process. It is found [6] that if the yield stress of the resin measured in compression, σ_y, is high then crack propagation is continuous, whereas if σ_y falls due to changes in the composition of the resin or testing variables then propagation tends to be stick/slip in nature. This behaviour is illustrated in Fig. 8 where K_{ICi} is plotted against σ_y for a whole range of Epikote 828/TETA formulations tested at different rates and temperatures. The values of σ_y have been taken from Part 1 and those of K_{ICi} from this and previous publications. It can be seen that all of the data fall approximately upon a master curve indicating a unique relationship between K_{ICi} and σ_y. It has recently been possible to explain this behaviour quantitatively in terms of a crack blunting process [8–10].

It can be shown [20] that for a crack under an applied stress of σ_o, the stress σ_{yy} normal to the axis of the crack at a small distance r ahead of the crack tip is given by

$$\sigma_{yy} = \frac{\sigma_o \sqrt{a}}{\sqrt{(2r)}} \frac{(1 + \rho/r)}{(1 + \rho/2r)^{3/2}} \qquad (2)$$

where ρ is the crack tip radius and a is the crack length. If it is postulated that fracture occurs when a critical stress σ_c is reached at a distance $r = c$ then Equation 2 can be written as

$$\frac{\sigma\sqrt{(\pi a)}}{\sigma_c\sqrt{(2\pi c)}} = \frac{(1 + \rho/2c)^{3/2}}{(1 + \rho/c)} . \qquad (3)$$

The term $\sigma_c \sqrt{(2\pi c)}$ can be considered as the critical stress intensity factor for a "sharp" crack K_{IC} [20] and $\sigma \sqrt{(\pi a)}$ as the stress intensity factor for a blunt crack, K_{IB} [20]. Hence

$$\frac{K_{IB}}{K_{IC}} = \frac{(1 + \rho/2c)^{3/2}}{(1 + \rho/c)} . \qquad (4)$$

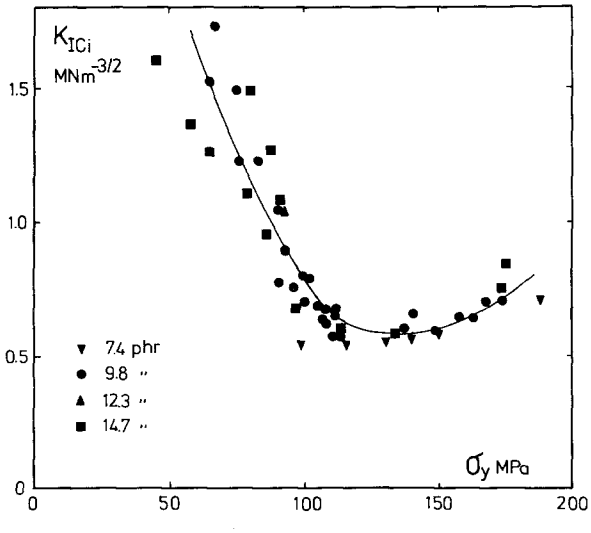

Figure 8 Plot of K_{ICi} against σ_y for different formulations of resin tested at a variety of rates and temperatures. The values of σ_y have been taken from Part 1.

This equation relates K_{IB} for a blunted crack to the crack tip radius ρ. It has already been suggested that blunting occurs during stick/slip propagation in epoxy resins [6] but it is very difficult to measure ρ directly. Kinloch and Williams [10] overcame this problem by measuring K_{IB} as a function of ρ for a series of epoxy resin samples containing blunt cracks which had been formed by drilled holes of known diameter at a crack tip. They showed very clearly that a relationship of the form of Equation 4 holds extremely well for these materials.

Yamini and Young [9] suggested that it might be appropriate to take ρ equal to r_p but Kinloch and Williams [10] showed that it might be more reasonable to take ρ equal to the crack opening displacement, δ_t. They also showed that extrapolation of the relationship between K_{IB} and ρ for artifically drilled holes would be consistent with this approximation. It was suggested in Section 4.2 that there is strong evidence that there is a Dugdale plastic zone at the crack tip during stick/slip propagation and so we have taken ρ to be equal to δ_t using the standard relationship for a Dugdale plastic zone [21]

$$\rho \simeq \delta_t = e_y \left(\frac{K_{IB}}{\sigma_y}\right)^2 \qquad (5)$$

where e_y is the yield strain of the material. It is possible then to estimate ρ using Equation 5 and so predict K_{IB}/K_{IC} for given values of c.

The theory can be tested by measuring the ratio K_{IB}/K_{IC} as a function of ρ over a wide range of temperature which produces large changes in the values of these parameters. This has been done using the data in Fig. 1 for the resins containing 9.8 and 14.7 phr hardener. The yield data for these materials are given in Part 1.

The data points in Fig. 9 are the values of K_{IB}/K_{IC} measured as a function of $(\rho/2c)^{1/2}$ for the two formulations of resin. K_{IC} has been taken arbitrarily as the value of K_{IC} at the lowest temperature used ($-60°$ C) and K_{IB} as the value of K_{ICi} at higher temperatures. The value of ρ has been calculated using Equation 5 and the appropriate values of K_{IB} ($=K_{ICi}$) and σ_y (Part 1). Ideally the same strain rates should be used for both K_{ICi} and σ_y. In fact, the same cross-head speeds have been used instead. It is envisaged that the error caused by this approximation will be only small. The solid lines are the relationship between K_{IB}/K_{IC} and $(\rho/2c)^{1/2}$ predicted using

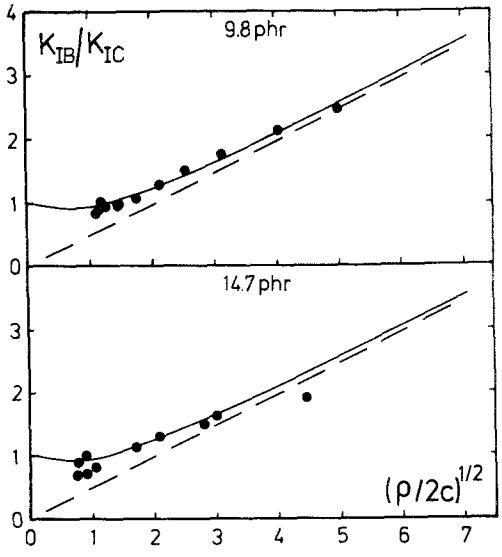

Figure 9 (K_{IB}/K_{IC}) as a function of $(\rho/2c)^{1/2}$. The value of ρ has been taken as δ_t as given by Equation 5. The experimental points have been fitted to the theoretical (solid) curve by assuming the values of c given in Table I. The curve is assymptotic to the dashed line of slope $= \frac{1}{2}$.

Equation 4 and they are assymptotic to the dashed lines since as $\rho/c \to \infty$ then $(K_{IB}/K_{IC}) \to \frac{1}{2}(\rho/2c)^{1/2}$. The data points in Fig. 9 are fitted to the theoretical curves by choosing appropriate values of c which is the only adjustable parameter. The values of critical distance, c, used for the data in Fig. 9 are 0.6 and 1.6 μm for the 9.8 and 14.7 phr TETA resins, respectively. Once the value of c has been determined, it is possible to calculate the value of critical stress σ_c using the relationship $K_{IC} = \sigma_c\sqrt{(2\pi c)}$. The values of c and σ_c for the TETA-cured resins are given in Table I for the two sets of data in Fig. 9 and for similar calculations on the resin cured with 12.3 phr TETA described in an earlier publication [7]. Kinloch and Williams [10] obtained values of c and σ_c for a series of resins cured with different hardeners but did not look at the effect of varying the amount of hardener. It can be clearly seen that increasing the amount of hardener causes a large increase in the critical distance, c and a small reduction in σ_c. It was shown in Part 1 that an increase in the amount of curing agent in the resin caused a reduction in the yield stress of the resin at a given strain rate and testing temperature. Values of σ_y at 25° C for the three formulations are also given in Table I and it can be seen that the ratio σ_c/σ_y for each one is remarkably constant (~ 3.2). The temperature of 25° C is only an arbitrary reference but the constant

TABLE I Derived values of c and σ_c for the epoxy resins of different formulations. The values of σ_y at 25° C have been taken from Part 1.

phr TETA	c (μm)	σ_c (MPa)	σ_y (25° C) (MPa)	σ_c/σ_y
9.8	0.6	360	112	3.2
12.3	1.1	300	91	3.3
14.7	1.6	270	86	3.2

ratio implies that the failure criterion is that a stress of the order of three times the yield stress must be reached in the plastic zone for failure to occur, regardless of the resin composition or yield stress. Inspection of the data of Kinloch and Williams [10] has shown that this is also probably the case for the different systems that they investigated.

4.4. Adiabatic/isothermal transition

There have recently been suggestions [22] that the transition from continuous to stick/slip crack propagation in epoxy resins is due to an adiabatic/isothermal transition. This type of mechanism has only been shown to be applicable in polymers for the situation of a fast-running crack with a single craze at the tip (e.g. PMMA [2]). The experimental observations strongly suggest that the adiabatic/isothermal mechanism cannot explain the crack propagation behaviour of epoxy resins. The most obvious example is that at a given temperature stick/slip propagation tends to occur as the rate of crack propagation is decreased whereas the adiabatic/isothermal transition in PMMA takes place when the rate of crack propagation is increased. The authors look forward with interest to the explanation of stick/slip behaviour in epoxy resins, through the adiabatic/isothermal mechanism, that has been promised [22].

5. Conclusions

It has been shown that crack propagation behaviour in epoxy resins is controlled by the plastic deformation characteristics of the material. The stick/slip propagation that is found in certain formulations tested at high temperatures has been shown to be caused by a crack blunting mechanism. A unique failure criterion has been shown to apply for the epoxy system studied. The criterion is that failure occurs when a critical stress of the order of three times the yield stress of the resin must be achieved at a critical distance ahead of the crack.

It has also been shown that the slow-growth region that is found on fracture surfaces of specimens undergoing stick/slip behaviour is of the same dimensions as that expected for a Dugdale line plastic zone and it seems that the region is caused by the slow growth of a crack through the plastic zone before it accelerates rapidly through virgin material.

No evidence has been found for crazing in epoxy resins from optical investigations or by taking fracture surface replicas and examining them in an electron microscope. An underlying nodular structure can be resolved from the replicas and it is found that for a given amount of curing agent the average nodule size decreases as the curing temperature is increased. However, there is no evidence of any direct correlation between the nodule size and the fracture behaviour of the materials.

Acknowledgements

The authors are grateful to Professor J. G. Williams and Dr A. J. Kinloch for useful discussions and suggestions throughout the course of this work and to Dr Kinloch for reading the manuscript. The project was supported by a research grant from the Science Research Council.

References

1. R. J. YOUNG, "Development in Polymer Fracture", edited by E. H. Andrews (Applied Science Publishers, London, 1979) Ch. 6.
2. G. P. MARSHALL, L. H. COUTTS and J. G. WILLIAMS, *J. Mater. Sci.* 9 (1974) 1409.
3. R. J. YOUNG and P. W. R. BEAUMONT, *Polymer* 17 (1976) 717.
4. *Idem, J. Mater, Sci.* 11 (1976) 776.
5. S. YAMINI and R. J. YOUNG, *Polymer* 18 (1977) 1075.
6. R. A. GLEDHILL, A. J. KINLOCH, S. YAMINI and R. J. YOUNG, *ibid* 19 (1978) 574.
7. S. YAMINI and R. J. YOUNG, *J. Mater. Sci.* 14 (1979) 1609.
8. J. G. WILLIAMS, private connumication.
9. R. J. YOUNG and S. YAMINI, paper presented at IUPAC Symposium on Macromolecules, Mainz (1979).
10. A. J. KINLOCH and J. G. WILLIAMS, *J. Mater. Sci.* 15 (1980) 987.
11. P. W. R. BEAUMONT and R. J. YOUNG, *ibid* 10

(1975) 1334.
12. S. YAMINI, Ph.D. Thesis, University of London (1979).
13. D. C. PHILLIPS, J. M. SCOTT and M. JONES, *J. Mater Sci.* **13** (1978) 311.
14. R. J. MORGAN and J. E. O'NEAL, *ibid* **12** (1977) 1966.
15. J. LILLEY and D. G. HOLLOWAY, *Phil. Mag.* **28** (1973) 215.
16. J. MIJOVIC and J. A. KOUTSKY, *Polymer* **20** (1978) 1095.
17. J. L. RACICH and J. A. KOUTSKY, *J. Appl. Polymer Sci.* **20** (1976) 2111.
18. D. R. UHLMANN, *Discuss. Faraday Soc.* 68 (1978).
19. G. S. YEH, *Crit. Rev. Macromol. Chem.* **1** (1972) 173.
20. J. G. WILLIAMS, "Stress Analysis of Polymers" (Longmans, London 1973).
21. J. G. WILLIAMS, *Adv. Polymer Sci.* **27** (1978) 69.
22. Y. W. MAI and N. B. LEETE, *J. Mater Sci.* **14** (1979) 2264.

Received 20 November and accepted 17 December 1979.